# A Spectroscopic Study of Diphenylmethyl Radicals and Diphenylmethyl Carbocations Stabilized by Zeolites

**Steffen Jockusch, Takashi Hirano,† Zhiqiang Liu, and Nicholas J. Turro***

*Department of Chemistry, Columbia University, New York, New York 10027*

*Received: August 23, 1999; In Final Form: November 10, 1999*

Photolysis of tetraphenylacetone on LZ-105 zeolites leads to diphenylmethyl radicals. Diffuse reflectance laser flash photolysis showed that most of the radicals decayed in the microsecond time scale. However, approximately 2−7% of the diphenylmethyl radicals remained as persistent radicals probably inside the zeolite channels with lifetimes of the order of weeks. The persistent radicals were detected by steady-state diffuse reflectance and steady-state and time-resolved fluorescence spectroscopy. In addition to the diphenylmethyl radicals, stable diphenylmethyl carbocations were formed and were detected by steady-state diffuse reflectance and steady-state and time-resolved fluorescence spectroscopy.

## Introduction

From the first preparation of a carbon-centered radical, triphenylmethyl radical (TPM•), by Gomberg in 1900, radical chemistry has spread to include studies of their reactivity as well as their spectroscopic characterization.[1,2] One of the advantageous properties of TPM• is their persistence, which has been categorized by Griller and Ingold.[3] In addition to a resonance stability obtained by the phenyl groups, the latter also inhibit radical−radical recombination reactions by an intramolecular steric effect to render TPM• persistent. This intramolecular steric effect has been shown to be the main structural source of the persistence of TPM•. The radicals in the arylmethyl family, which includes TPM•, have progressively contributed to the photophysical and photochemical studies of radicals because their preparation and characterization are easier than those of simple alkyl radicals. Therefore, the spectroscopic properties of benzyl,[4−6] diphenylmethyl,[6−10] and triphenylmethyl radicals[6,10,11] have been extensively studied under various molecular conditions. From the viewpoint of zeolite chemistry, benzyl and diphenylmethyl radicals (DPM•) have simple structures and molecular dimensions that fit the channel size of a MFI zeolite. By using this matching of sizes, we have achieved a preparation of supramolecularly persistent DPM• generated photochemically on the sodium form of LZ-105, a MFI zeolite (Scheme 1).[12,13] 1,1,3,3-Tetraphenylacetone (TPA) was employed as an efficient precursor of DPM•.[7,14−16]

As shown in eq 1, photolysis of TPA leads to α-cleavage forming diphenylacetyl radicals and diphenylmethyl radicals. Decarbonylation of the diphenylacetyl radical proceeds within 10 ns to form a second DPM•.[16] In a fluid solution at room temperature, DPM• undergoes nearly diffusion-controlled, radical−radical coupling to quantitatively form 1,1,2,2-tetraphenylethane.[14,17] However, inside the channels of LZ-105 the mobility of DPM• is restricted. Radical−radical recombinations are inhibited, leading to persistent DPM• which can be observed with a half-life of many weeks at room temperature.[18,19] Our

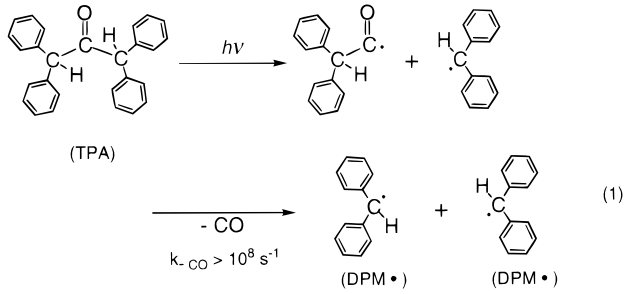


(1)

previous studies focused on the detection via EPR spectroscopy of supramolecularly persistent DPM• adsorbed on LZ-105.[18] In this work, to evaluate in detail the effect of a newly employed supramolecular environment on radical character, the spectroscopic properties of DPM• adsorbed on LZ-105 were investigated with optical absorption and emission spectroscopy.

## Experimental

1,1,3,3-Tetraphenylacetone (TPA) was synthesized as previously described.[18] TPA was adsorbed on the external surface of LZ-105 from isooctane solutions at 0.1−0.5% loading (w/w). After removal of the solvent by evaporation under a steady stream of argon, the sample was further degassed under vacuum (ca. $5 \times 10^{-5}$ Torr). Steady-state photolysis of the evacuated dry zeolite powder loaded with TPA was performed by tumbling the quartz vessel in front of a 450 W medium-pressure Hg lamp (Hanovia). The light was filtered through a $K_2CrO_4$ filter solution to achieve a band-pass of approximately 290−330 nm.[20] For optical measurements, a quartz vessel with a branch containing a rectangular quartz cell (10 mm × 1 mm) was employed.

Steady-state optical diffuse reflectance spectra (remission function)[21,22] were recorded on a Lambda 6 spectrometer (Perkin-Elmer) using an integrating sphere attachment. Steady-state fluorescence emission and excitation spectra were recorded on a Fluorolog 1680 0.22-m double spectrometer (SPEX). Time-resolved fluorescence measurements were performed by single photon counting on a OB900 fluorometer (Edinburgh Analytical Instruments). Diffuse reflectance laser flash photolysis experi-

* To whom correspondence should be addressed. E-mail: turro@chem.columbia.edu.

† Present address: The University of Electro-Communications, Department of Applied Physics and Chemistry, Chofu, Tokyo 182, Japan.

10.1021/jp992978s CCC: $19.00 
Published on Web 01/26/2000

**SCHEME 1: Schematic Representation of the Dimensions of LZ-105 and DPM•**

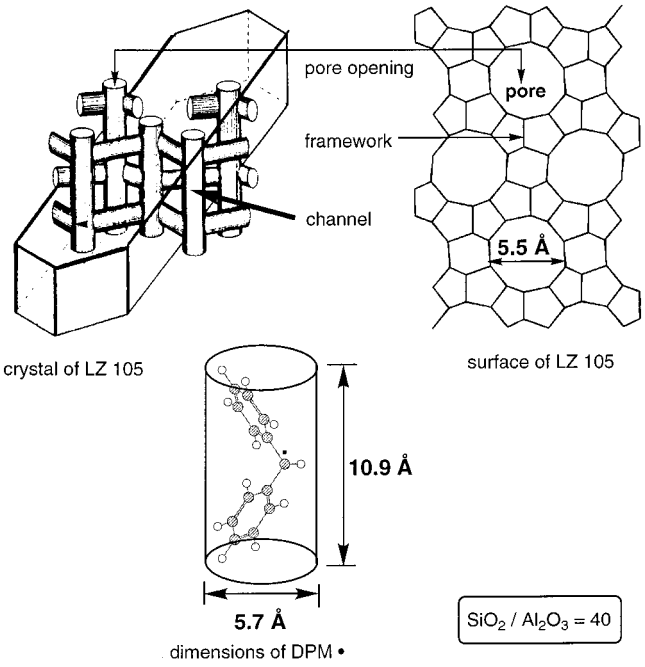


ments employed the pulses (266, ca. 4 mJ/pulse, 8 ns) from a Spectra Physics GCR-150-30 Nd:YAG laser and a computer-controlled system that has been described elsewhere.[23] The optical configuration was similar to that used by Wilkinson and Kelly.[22] The data analysis was based on the fraction of reflected light absorbed by the transient (reflectance change ($\Delta J/J_o$) where $J_o$ is the reflectance intensity before laser excitation and $\Delta J$ is the change in the reflectance after excitation.

## Results and Discussion

**Steady-State Diffuse Reflectance Spectroscopy.** The remission function[21,22] of an evacuated dry powder sample of TPA on LZ-105 (0.1% loading) was measured by employing an integrating sphere. It showed some optical absorption below 350 nm due to the absorption of TPA. This spectrum was used as a baseline for the spectra shown in Figure 1. The zeolite sample was then irradiated for 15 min with a 450 W medium-pressure Hg lamp. The baseline-corrected remission function is shown in Figure 1a. The spectrum features two maxima at 325 and 433 nm. The absorption centered at 325 nm corresponds to the DPM• and is in good agreement with previously published absorption spectra of DPM• in a glass matrix at 77 K[24] and transient absorption spectra at room temperature.[7,9,11,25] After exposure of the zeolite sample to air, the absorption at 325 nm immediately disappeared (Figure 1b) by a reaction with oxygen (eq 3) ($k_{oxygen} = 6.3 \times 10^8$ $M^{-1}$ $s^{-1}$).[8] This reactivity with oxygen is in agreement with the reactivity of DPM• on LZ-105 observed by EPR to form peroxy radicals.[19] Evacuation of the sample below $1 \times 10^{-4}$ Torr recovered some of the DPM• from the peroxy radicals (Figure 1c). This reversible oxygenation reaction of DPM• observed by absorption spectroscopy matches the results observed by EPR and fluorescence spectroscopy.[19]

Figure 1a shows another absorption with maximum at 433 nm, which was assigned to the absorption band of the diphenylmethyl carbocation ($DPM^+$). A similar absorption was observed by dehalogenation of diphenylmethyl chloride by laser excitation ($\lambda_{max} = 435$ nm in acetonitrile solution).[11] In addition, we found that $DPM^+$ could also be generated thermally by a

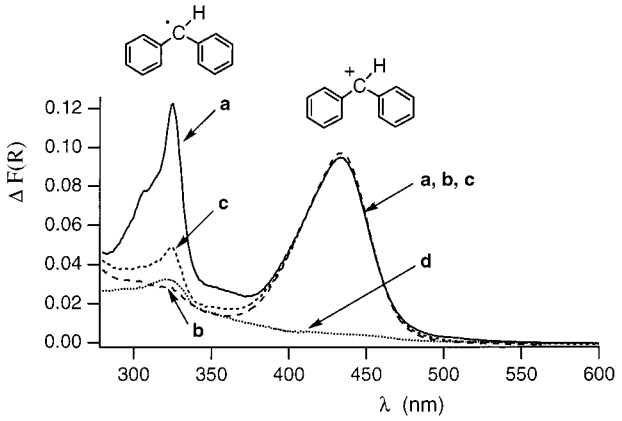


**Figure 1.** Steady-state diffuse reflectance (remission function) difference spectra of TPA (0.1% loading) on LZ-105 after 15 min of photolysis (313 nm) under vacuum (a); followed by addition of air (b); followed by evacuation (c); and followed by addition of methanol vapor under air (d).

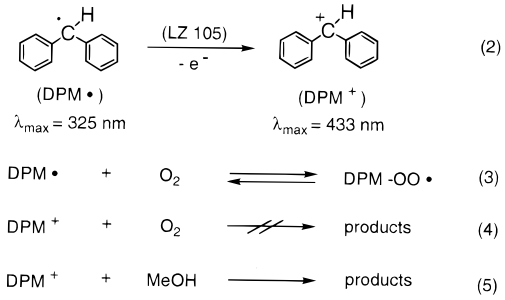


reaction of diphenylmethyl chloride with LZ-105 resulting from simple absorption. The diffuse reflectance spectrum of the thermally generated $DPM^+$ matched with that of $DPM^+$ generated during the photoreaction of TPA on LZ-105. $DPM^+$ could be formed by electron loss of the DPM• in LZ-105 (eq 2). Oxidation reactions of organic compounds adsorbed on zeolites have been commonly observed.[26−28] Exposure of the zeolite sample to air did not quench the carbocation absorption (Figure 1b). This reactivity of $DPM^+$ on LZ-105 is consistent with the low reactivity of carbocations toward oxygen (eq 4).[11] In contrast, the addition of methanol vapor quenched the $DPM^+$ absorption completely (Figure 1d). This is in agreement with the high rate constant of the reaction of the carbocation with methanol (eq 5) ($k_{MeOH} = 1.2 \times 10^9$ $M^{-1}$ $s^{-1}$; in acetonitrile solution).[29]

**Steady-State Fluorescence Spectroscopy.** An evacuated dry zeolite powder sample containing 0.3% of TPA on LZ-105 was irradiated for 30 min with a Hg lamp. Excitation at 325 nm led to an emission spectrum with a maximum at 512 nm (Figure 2), which corresponds to the doublet−doublet fluorescence of the DPM•.[7,9,10] The excitation spectrum of this emission (Figure 2) is in good agreement with the diffuse reflectance spectrum of the DPM• (Figure 1a). In addition to the fluorescence of DPM•, the fluorescence of the $DPM^+$ was also observed when the photolyzed zeolite sample was excited at 432 nm, where the carbocation is expected to absorb strongly (see Figure 1a). Excitation at 432 nm gave an emission spectrum centered at 550 nm, but its excitation spectrum was dominated by the spectral features of the DPM•, which suggests that the fluorescence quantum yield of $DPM^+$ is much lower than that of DPM•. In the presence of air (equivalent to the condition in Figure 1b), the DPM• were scavenged by oxygen completely (eq 3), and the fluorescence emission ($\lambda_{max} = 551$ nm) and excitation ($\lambda_{max} = 432$ nm) spectra of the $DPM^+$ were clearly observed

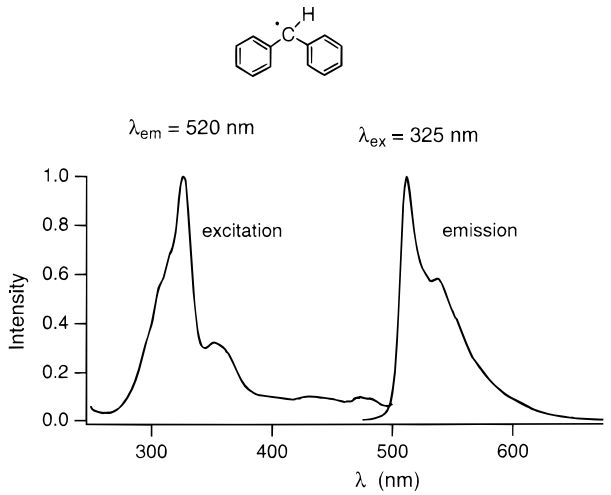


**Figure 2.** Steady-state fluorescence excitation ($\lambda_{em}$ = 520 nm) and emission ($\lambda_{ex}$ = 325 nm) spectra of photolyzed (30 min at 313 nm) TPA on LZ-105 (0.3% loading).

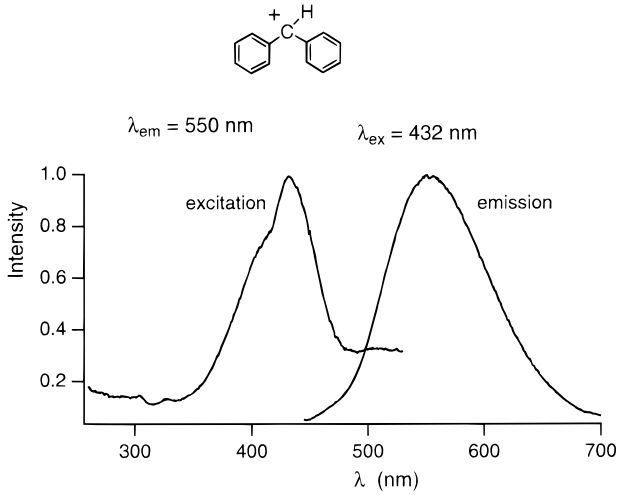


**Figure 3.** Steady-state fluorescence excitation ($\lambda_{em}$ = 550 nm) and emission ($\lambda_{ex}$ = 432 nm) spectra of photolyzed (30 min at 313 nm) TPA on LZ-105 (0.3% loading) after exposure to air.

without interference from the DPM• emission (Figure 3). The excitation spectrum is in good agreement with the diffuse reflectance spectrum observed for the $DPM^+$ (Figure 1a−c).

**Time-Resolved Fluorescence Spectroscopy.** By time-correlated single photon counting, the time-resolved emission spectra were collected for photolyzed TPA on LZ-105 under degassed conditions. The time-resolved fluorescence spectrum of the DPM•, observed 10−100 ns after the lamp pulse at $\lambda_{ex}$ = 325 nm, is shown in Figure 4 and is in good agreement with the steady-state fluorescence spectrum (Figure 2). The emission decay follows approximately first-order kinetics with a lifetime of around 300 ns. Distribution analysis of this decay, using the maximum entropy method, revealed distribution of lifetimes over an approximately 500-ns range centered at 314 ns. A broad distribution of lifetimes is expected, since zeolites are considered to be an inhomogeneous system. Broad lifetime distributions of excited states of guest molecules in zeolites were reported frequently.[30] The order of the fluorescence lifetime in LZ-105 is similar to a reported value for DPM• in homogeneous solution (278 ns in acetonitrile).[10]

Figure 5 shows the time-resolved emission spectrum of the $DPM^+$ observed 2.5 ns following the lamp pulse at $\lambda_{ex}$ = 432 nm. It is in good agreement with the steady-state fluorescence

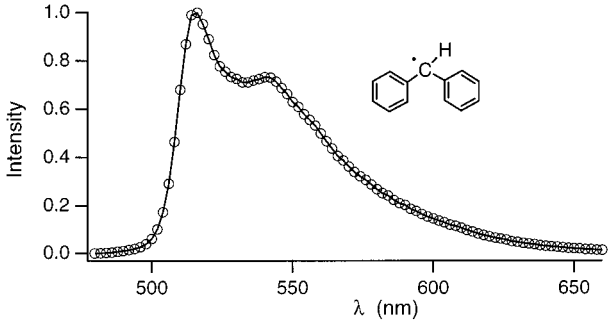


**Figure 4.** Time-resolved emission spectrum recorded 10−100 ns after the lamp pulse ($\lambda_{ex}$ = 325 nm) of photolyzed (30 min at 313 nm) TPA on LZ-105 (0.3% loading).

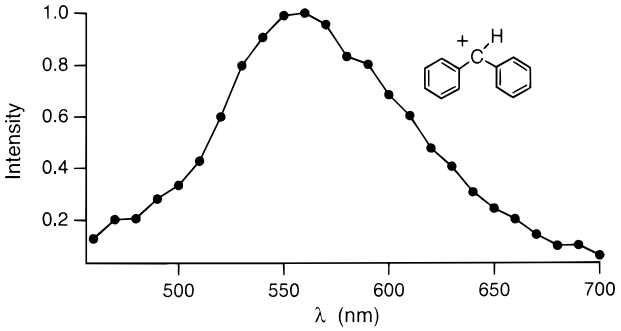


**Figure 5.** Time-resolved emission spectrum recorded 0−2.5 ns after the lamp pulse ($\lambda_{ex}$ = 432 nm) of photolyzed (30 min at 313 nm) TPA on LZ-105 (0.3% loading).

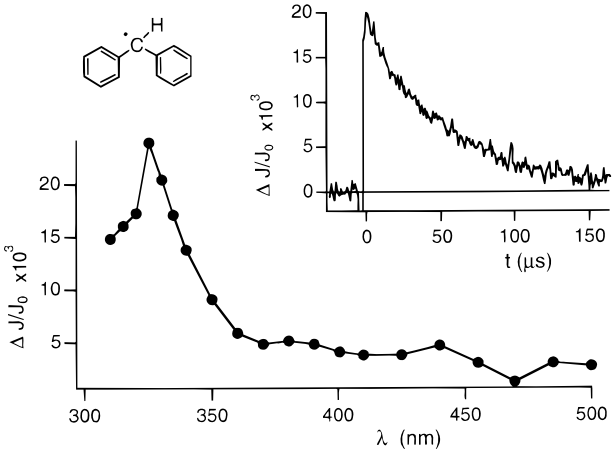


**Figure 6.** Transient diffuse reflectance spectrum recorded 5−45 $\mu$s following laser excitation (266 nm, 8 ns) of TPA on LZ-105 (0.5% loading). Inset: Transient decay kinetic at 330 nm.

spectrum shown in Figure 3. At a longer time scale the time-resolved emission spectrum is dominated by the fluorescence of the DPM•. Kinetic analysis of the signal decay showed a fluorescence lifetime of the $DPM^+$ of approximately 8 ns.

**Diffuse Reflectance Laser Flash Photolysis.** Steady-state diffuse reflectance and steady-state and time-resolved fluorescence spectroscopy can be used only to observe persistent radicals or persistent carbocations. To look at a time scale for radical formation during the photolysis of TPA (eq 1), diffuse reflectance laser flash photolysis was employed. Evacuated samples of TPA loaded on LZ-105 (0.5%) were irradiated with laser pulses (266 nm, 8 ns). The transient diffuse reflectance spectrum recorded 5−45 $\mu$s following the laser flash is shown in Figure 6. This spectrum, which possesses a maximum at about 325 nm, was correlated to the DPM• and matches well with the steady-state spectrum (see Figure 1).

The inset in Figure 6 shows the transient decay observed at 330 nm and follows roughly first-order kinetics ($\tau = 44$ $\mu$s). Product analysis of the photoreaction of TPA adsorbed on LZ-105 showed a 40−50% yield of 1,1,2,2-tetraphenylethane, the product generated by a radical recombination.[18] Although second-order kinetics for a radical recombination reaction is expected in fluid solutions, it is known that solution chemistry rules are not applicable on surfaces, where molecules have restricted freedom of movement.[31] In zeolite NaX, for instance, a complex decay kinetics for DPM$^\bullet$ generated photochemically from TPA was observed.[32] Because NaX possesses larger cavities (13 Å) and wider channels (8 Å) than those of LZ-105, the DPM$^\bullet$ are able to move more freely inside the channels of NaX than in the channels of LZ-105 (5.5 Å, Scheme 1). In addition, TPA would be able to diffuse inside the cavities of NaX, and most of the photocleavage of TPA (eq 1) and subsequent recombination of DPM$^\bullet$ would also occur inside the cavities. In the case of LZ-105, however, TPA is adsorbed on the external surface, especially at the external surface pore opening, which are entrances into the LZ-105 channels. Therefore, photolysis of TPA occurs outside the channels, and subsequently DPM$^\bullet$ are generated on the LZ-105 surface. Most of the recombination of DPM$^\bullet$ would occur on the external surface, to give 1,1,2,2-tetraphenylethane in 40−50% yield. DPM$^\bullet$ able to escape from the pore openings into the LZ-105 channels on the internal surface become persistent with a long lifetime and should possess a low probability for encounter to give recombination products. Another possible decay process of DPM$^\bullet$ located in the LZ-105 channels would be oxidation to give DPM$^+$. Consequently, these reaction pathways of DPM$^\bullet$ adsorbed on LZ-105 are responsible for the complex decay kinetics.

During the observation time in laser flash photolysis experiments, the transient decayed to an approximately 2% residual. This is consistent with the formation of persistent radicals, which were observed by steady-state techniques described above.

Previously, it was shown that TPA loadings below 0.3% produced higher yields of persistent radicals than those loadings above 0.3%.[18] This was explained by the predominant location of TPA at the pore openings of the zeolite. Above 0.3% loading, all the pore openings are covered and TPA becomes located on the external surface between the pore openings. It was shown that persistent DPM$^\bullet$, which are probably inside the zeolite channels, originate from TPA located on the zeolite pore openings.[18] Accordingly, in the laser flash experiments, decreased loading of TPA on LZ-105 should increase the yield of persistent radicals, which should be reflected by the residual absorption after the transient decayed. But no major increase of the residual absorption was observed at 0.1% loading within the accuracy of our instrumental setup. Only the lifetime of the fast-decaying component of DPM$^\bullet$ increased slightly from 44 to 62 and 69 $\mu$s (0.5%, 0.3%, and 0.1% loading, respectively). This can be explained by the lower radical concentration at lower loadings generated by one laser flash.

The yield of persistent radicals generated by photolysis of TPA on LZ-105 (0.1% loading) was also estimated by EPR spectroscopy as approximately 4−7%.[33] This is slightly higher than the amount of residual absorption observed by laser flash photolysis and can be explained by the higher local concentration of radicals in the laser experiments compared to steady-state irradiation for the EPR experiments. High local radical concentration renders encounter for recombinations more likely before the radicals can escape into the zeolite channels.

A significant formation of DPM$^+$ could not be detected by diffuse reflectance laser flash photolysis within the observation time scale of our experimental setup. The DPM$^+$ are probably produced on much longer time scales by an oxidation mechanism involving a fraction of DPM$^\bullet$ inside the LZ-105 channels. Recently, oxidation reactions of some organic molecules in zeolite channels and cavities have been observed.[26−28] The exact reaction mechanisms remain unsolved. The generation of DPM$^+$ from DPM$^\bullet$ in the LZ-105 channels might be an experimental system to clarify this mechanism.

## Summary and Conclusion

Photolysis of TPA adsorbed on LZ-105 leads to DPM$^\bullet$ and DPM$^+$. Diffuse reflectance laser flash photolysis showed that most of the radicals decayed within the microsecond time scale. Approximately 2−7% of the DPM$^\bullet$ remained as persistent DPM$^\bullet$, probably located inside the LZ-105 channels. Persistent DPM$^\bullet$ were also detected by steady-state diffuse reflectance and steady-state and time-resolved fluorescence spectroscopy. In addition to the DPM$^\bullet$, stable DPM$^+$ were also observed and were characterized by steady-state diffuse reflectance and steady-state and time-resolved fluorescence spectroscopy.

**Acknowledgment.** We thank the National Science Foundation for Grant CHE98-12676. This work was also supported in part by the National Science Foundation and the Department of Energy under Grant No. NSF CHE98-10367 to the Environmental Molecular Sciences Institute (EMSI) at Columbia University.

## References and Notes

(1) Gomberg, M. *Ber. Dtsch. Chem. Ges.* **1900**, *33*, 3150−3163.
(2) Gomberg, M. *J. Am. Chem. Soc.* **1900**, *22*, 757−771.
(3) Griller, D.; Ingold, K. U. *Acc. Chem. Res.* **1976**, *9*, 13−19.
(4) Mittal, J. P.; Hayon, E. *Nat. Phys. Sci.* **1972**, *240*, 20−21.
(5) Claridge, R. F. C.; Fischer, H. *J. Phys. Chem.* **1983**, *87*, 1960−1967.
(6) Meisel, D.; Das, P. K.; Hug, G. L.; Bhattacharyya, K.; Fessenden, R. W. *J. Am. Chem. Soc.* **1986**, *108*, 4706−4710.
(7) Kelly, G.; Willsher, C. J.; Wilkinson, F.; Netto-Ferreira, J. C.; Olea, A.; Weir, D.; Johnston, L. J.; Scaiano, J. C. *Can. J. Chem.* **1990**, *68*, 812−819.
(8) Scaiano, J. C.; Tanner, M.; Weir, D. *J. Am. Chem. Soc.* **1985**, *107*, 4396−4403.
(9) Bromberg, A.; Schmidt, K. H.; Meisel, D. *J, Am Chem. Soc.* **1984**, *106*, 3056−3057.
(10) Bromberg, A.; Schmidt, K. H.; Meisel, D. *J. Am. Chem. Soc.* **1985**, *107*, 83−91.
(11) Bartl, J.; Steenken, S.; Mayr, H.; McClelland, R. A. *J. Am. Chem. Soc.* **1990**, *112*, 6918−6928.
(12) Meier, W. M.; Olson, D. H. *Atlas of Zeolite Structure Types*; Butterworth-Heinemann: London, 1992.
(13) Davis, M. E.; Lobo, R. F. *Chem. Mater.* **1992**, *4*, 756−768.
(14) Quinkert, G.; Opitz, K.; Weirdorff, W. W.; Weinlich, J. *Tetrahedron Lett.* **1963**, 1863−1868.
(15) Gould, I. R.; Zimmt, M. B.; Turro, N. J.; Baretz, B. H.; Lehr, G. F. *J. Am. Chem. Soc.* **1985**, *107*, 4607−4612.
(16) Gould, I. R.; Baretz, B. H.; Turro, N. J. *J. Phys. Chem.* **1987**, *91*, 925−929.
(17) Quinkert, G. *Pure Appl. Chem.* **1964**, *9*, 604−621.
(18) Hirano, T.; Li, W.; Abrams, L.; Krusic, P. L.; Ottaviani, M. F.; Turro, N. J. *J. Org. Chem.* **1999**, in press.
(19) Hirano, T.; Li, W.; Abrams, L.; Krusic, P. L.; Ottaviani, M. F.; Turro, N. J. *J. Am. Chem. Soc.* **1999**, *121*, 7170−7171.
(20) Murov, S. L.; Carmichael, I.; Hug, G. L. *Handbook of Photochemistry*, 2nd ed.; Marcel Dekker: New York, 1993.
(21) Kubelka, P. *J. Opt. Soc. Am.* **1948**, *38*, 448.
(22) Wilkinson, F.; Kelly, G. In *CRC Handbook of Organic Photochemistry*; Scaiano, J. C., Ed.; CRC Press: Boca Raton, FL, 1989; Vol. 1, p 293.

(23) McGarry, P. F.; Cheh, J.; Ruiz-Silva, B.; Hu, S.; Wang, J.; Nakanishi, K.; Turro, N. *J. Phys. Chem.* **1996**, *100*, 646−654.
(24) Bromberg, A.; Meisel, D. *J. Phys. Chem.* **1985**, *89*, 2507−2513.
(25) Hadel, L. M.; Platz, M. S.; Scaiano, J. C. *J. Am. Chem. Soc.* **1984**, *106*, 283−287.
(26) Yoon, K. B. *Chem. Rev.* **1993**, *93*, 321−339.
(27) Ramamurthy, V.; Caspar, J. V.; Corbin, D. R. *J. Am. Chem. Soc.* **1991**, *113*, 594−600.
(28) Lakkaraju, P. S.; Zhou, D.; Roth, H. D. *J. Chem. Soc., Perkin Trans. 2* **1998**, 1119−1121.
(29) Bartl, J.; Steenken, S.; Mayr, H. *J. Am. Chem. Soc.* **1991**, *113*, 7710−7716.
(30) Scaiano, J. C.; Kaila, M.; Corrent, S. *J. Phys. Chem. B* **1997**, *101*, 8564−8568.
(31) Barber, M. N.; Ninham, B. W. *Random and Restricted Walks*; Gordon and Breach: New York, 1970.
(32) Johnston, L. J.; Scaiano, J. C.; Shi, J.-L.; Siebrand, W.; Zerbetto, F. *J. Phys. Chem.* **1991**, *95*, 10018−10024.
(33) Unpublished results: The yield of persistent radicals in LZ-105 generated by photolysis of tetraphenylacetone (0.1% loading) was determined by EPR spectroscopy. The number of spins of DPM radicals was compared with 4-hydroxy-TEMPO loaded on LZ-105. The details will be the subject of an upcoming publication.